J Mater Sci (2007) 42:5406–5410
DOI 10.1007/s10853-006-0774-4

Preparation, spectroscopic properties and enhanced luminescence of Tb^{3+}-doped LuAG phosphors and transparent ceramics by introduction of Sc^{3+}

Yi-kun Liao · Dan-yu Jiang · Tao Feng · Na Zhang

Received: 7 June 2006 / Accepted: 8 August 2006 / Published online: 31 March 2007

Abstract Tb-doped LuAG(lutetium aluminum garnet) and LuSAG(lutetium scandium-aluminum garnet) precursors were synthesized through a co-precipitation process, using ammonium hydrogen carbonate as precipitator. Single-phase cubic LuAG/Tb and LuSAG/Tb phosphors were obtained after calcination at 1000 and 1200 °C, respectively. These powders could be easily sintered into corresponding transparent LuAG/Tb and LuSAG/Tb ceramics in H_2 atmosphere at 1850 °C. The PL excitation and emission spectra were recorded for both phosphors and ceramics. Emission spectra of all materials were found to be typical for Tb^{3+}, resulting from radiative relaxation of D level. Both the Tb-doped LuSAG phosphors and ceramics show higher efficient luminescence than LuAG , especially the transparent Tb-doped LuSAG ceramic shows about 150% higher luminescence intensity than transparent Tb-doped LuAG ceramic.

Introduction

The optical properties of trivalent terbium ions (Tb^{3+}) have been investigated extensively in a variety of host lattices. As is well known, the efficient blue-green emissions of Tb^{3+} originating from radiative relaxation of D level and Tb^{3+}-activated phosphors have been widely used in various application fields, such as projection television tubes (e.g., $Y_3(Al,Ga)_5O_{12}/Tb^{3+}$)[1], three-band fluorescent lamps (e.g., $(Ce,Gd)MgB_5O_{10}/Tb^{3+}$)[2], and X-ray intensifying screens (e.g. Gd_2O_2S/Tb^{3+})[3].

The $Lu_3Al_5O_{12}$(LuAG) has attracted considerable attention as host crystals for near-infrared solid-state lasers as well as for optoelectronics devices, including computer memories, microwave optical elements and as laser active media with applications in medical surgery, optical communications and coherent laser radar[4–6]. On the other hand, LuAG garnet crystals, due to their high density and other physical properties such as good shock resistance, non-hygroscopicity and chemical radiation stability, are known to be a promising host crystal for scintillating materials [7–9]. The largest effective atomic number and density make the LuAG garnet possess the highest X-ray absorption coefficiency among the known garnet compounds ($\eta_{abs} \approx \rho Z_{eff}^4$, where ρ is the density and Z_{eff} is the effective atomic number of the compound). However, due to the smallest ionic radius of the Lu^{3+} among all RE^{3+}(trivalent rare earth) ions, the solubility of other RE^{3+} ions (activators) in LuAG, especially large RE^{3+} ions, is relatively low. In an effort to find a solution to this problem, selective substitution of scandium(Sc), a large ion, into the octahedral site of aluminum in LuAG, is promising.

As an alternative, polycrystalline LuAG ceramic can be used as a substitute for single crystal LuAG because of its excellent scintillation performance, low-cost, short manufacturing period, and other characteristics, once high density and transparency can be made possible by synthesizing the LuAG powder and using transparent ceramic processing techniques. Recently, we successfully synthesized transparent RE^{3+}-doped LuAG and LuSAG ($Lu_3(Al,Sc)_5O_{12}$) ceramics. In this paper, we present the results of the preparation and optical properties of LuAG/Tb(5%) phosphors and ceramics. The effect of substitution of Sc^{3+} into

Y.-k. Liao (✉) · D.-y. Jiang · T. Feng · N. Zhang
R&D Center of Shanghai Institute of ceramics, Chinese Academy of Sciences, Shanghai 200050, P.R. China
e-mail: liaoyikun1@163.com

the octahedral site of alumina in LuAG/Tb on their crystalline behavior and spectroscopic properties are also discussed in detail.

Experimental

LuAG/Tb(5%) and LuSAG/Tb(5%) precursors were prepared by using analytical grade Lu_2O_3, Sc_2O_3, Tb_2O_3 and $Al(NO_3) \cdot 9H_2O$ as starting materials. NH_4HCO_3 of analytical grade was used as precipitator. Aqueous nitrate solutions of Lu^{3+}, Sc^{3+} and Tb^{3+} were prepared by dissolving corresponding metal oxide in diluted nitric acid (HNO_3) solution under stirring and heating. $Al(NO_3)_3$ solution was obtained by dissolving $Al(NO_3) \cdot 9H_2O$ in deionized water. The preparation of LuAG/Tb powder was completed in a simple coprecipitation process: The mixed nitrate solution containing Lu^{3+}, Al^{3+} and Tb^{3+} in the required ratio for $Tb_{0.15}Lu_{2.85}Al_5O_{12}$ was added at a speed of 2 ml min^{-1} into 2 M NH_4HCO_3 solution under mild stirring at room temperature. The resulting precipitate slurry was aged for 24 h, under the agitation by a supersonic cleaner. The precipitate was filtered and washed for three times with deionized water to remove the remaining ions. After washing and drying at 60 °C, the precursors were calcined in air for 2 h at different temperatures at a heating rate of 4°C min^{-1}. Then the powders were isostatically pressed at 180 MPa and finally the green pellets were sintered at 1850 °C for 6 h in a hydrogen atmosphere. The synthesis procedures of $Tb_{0.15}Lu_{2.85}Sc_2Al_3O_{12}$ phosphor and transparent ceramics are similar to that of LuAG/Tb.

The crystal phases of the powders and transparent ceramic were determined by X-ray diffraction (XRD) (Model D/MAX-C, Rigku, Tokyo, Japan) using Cu Kα radiation in the range of $2\theta = 10$–$70°$. Morphologies of the calcined powders were examined by SEM (FE-SEM, JSM-6700F, JEOL, Japan). The particle size of the powder was examined by TEM(Model JEM2010, JEOL, Japan). The excitation and emission spectra of as-prepared Tb-activated LuAG particles were measured using a fluorescence spectrophotometer (Perkin Elmer LS-55) with a xenon lamp as the excitation source. All the measurements were performed at room temperature (RT).

Results and discussion

XRD patterns of the LuAG/Tb(5%) and LuSAG/Tb(5%) powders calcined at various temperatures, are shown in Fig. 1. It is showed that the precursors of both types of materials obtained by the co-precipitation are amorphous. The diffraction pattern of LuAG/Tb calcined at 1000 °C shows the crystallized powder with all the peaks corresponding to the $Lu_3Al_5O_{12}$(LuAG) phase(JCPDS: 73-1368) and no other crystalline phases can be detected. However, the crystallization temperature of LuSAG/Tb is evidently 200 °C higher than that of LuAG/Tb. In addition, the diffraction patterns of both types of transparent ceramics were also shown in Fig. 1.

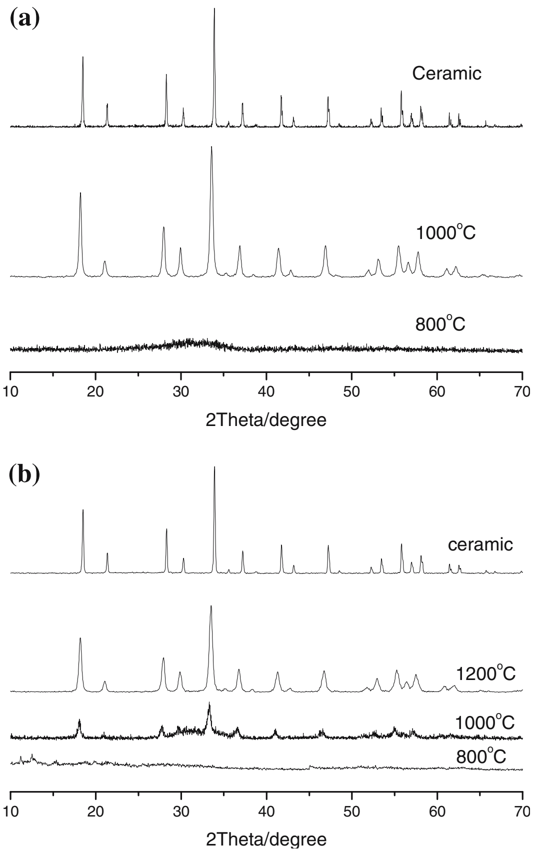

Fig. 1 XRD patterns of the precipitation-made powders calcined at different temperatures for 2 h: (**a**)LuAG/Tb; (**b**) LuSAG/Tb. Those of corresponding ceramics are also shown

The microstructures of 1000 °C-calcined LuAG/Tb and LuSAG/Tb powders are shown in Figs. 2 and 3. These samples are also the powders used for the preparation of corresponding transparent ceramics. We can hardly find the morphological differences between the two types of materials from these images. Weakly agglomerated crystallites with size in the range from 20 to 30 nm can be found for both types of powders. They also show uniform crystalline size and approximately spherical shape. These powders were found to be highly sinterable, near theoretical density can be achieved by sintering under H_2 atmosphere at 1850 °C. Although the LuSAG/Tb powder used for the preparation of transparent ceramic is still in amorphous state, subsequent sintering experiments suggest that this powder is equally highly sintering-active. Powder calcined at higher temperatures than 1000 °C shows strong

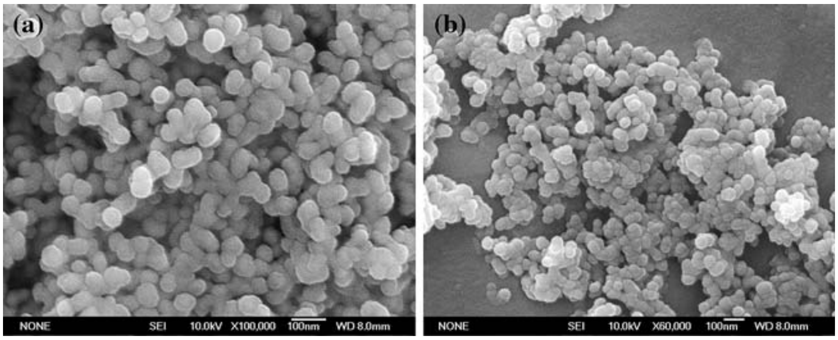

Fig. 2 SEM images of the powders calcined at 1000 °C for 2 h: (**a**) LuAG; (**b**) LuSAG

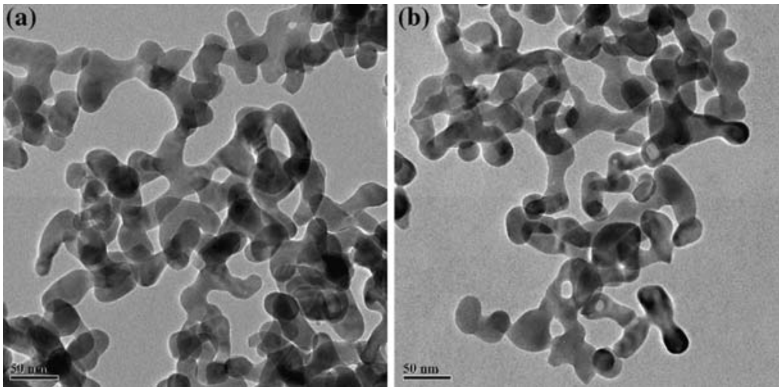

Fig. 3 TEM images of the powders calcined at 1000 °C for 2 h: (**a**) LuAG; (**b**) LuSAG

agglomeration between particles of larger size, and their sintering activity decreases accordingly.

Figure 4(a) shows the excitation spectra of the Tb^{3+} 544-nm emission in LuAG/Tb(5%) phosphor and LuAG/Tb(5%) transparent ceramic. The excitation spectrum of the phosphor consists of three bands, namely, a strong maximum at about 270 nm and two weak maxima located at 232 and 321 nm, respectively, which correspond to the Tb^{3+} 4f → 5d absorptions. The photoluminescence (PL) spectrum of phosphor excited under 270-nm UV excitation are shown in Fig. 4 (b). Only four obvious emission bands resulted from $^5D_4$–^7F_j transition of Tb^{3+} can be found from the emission spectra. The blue emission bands of the $^5D_3$–^7F_j transition disappeared due to the well-known cross-relaxation [10]. Compared with that of LuAG/Tb phosphor, the excitation spectrum of LuAG/Tb ceramic shows integrated red shift in addition to the enhancement of all peak intensity caused by the significant increased crystallinity and density of ceramics. In addition, it is also found that an asymmetrical broad band from 250 to 300 nm exists in the excitation spectrum of the ceramic. This broad band is mainly caused by another new peak at about 260 nm with overlaps with the peak at ~280 nm. The appearance of the new peak can be explained as follows. As the absorption coefficient for band-to-band transitions is always much higher than for the allowed transitions of 4f → 5d, the absorption band observed at ~260 nm could

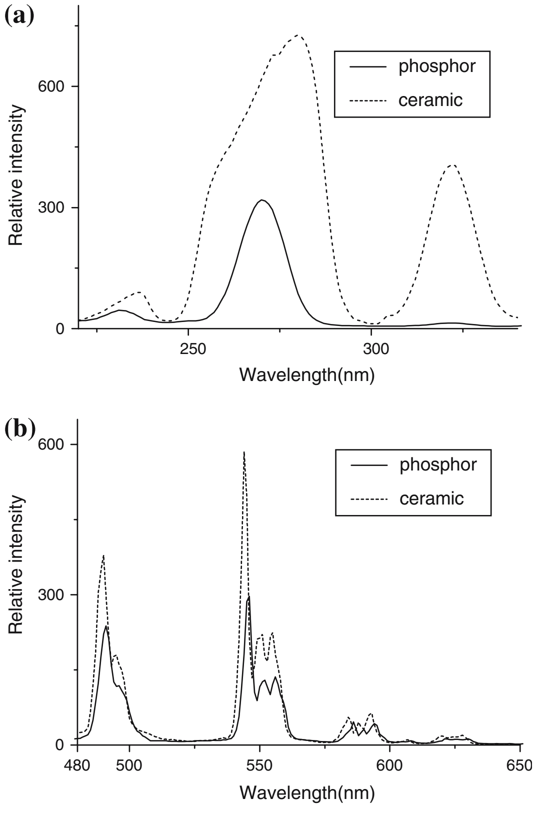

Fig. 4 Photoluminescence spectra of LuAG/Tb($Tb_{0.15}Lu_{2.85}Al_5O_{12}$): (**a**) excitation spectra(λ_{em}=544 nm); (**b**) emission spectra (λ_{ex}=270 nm)

then be inferred to be a kind of photoionization absorption of Tb^{3+}, namely, the electron of Tb^{3+} was ejected into the conduction band. Thus in the case of the transparent ceramic, the electrons in the conduction band due to photoionization of Tb^{3+} could be transferred to the Tb^{3+} more efficiently [11]. The complete crystallization, which lead to the significantly reduced surface effects of particles and the near perfect host periodic lattice accomplished during the high temperature sintering process, may favor such an energy transfer. The emission of the LuAG/Tb ceramic, when normalized, has a virtually identical shape with that of phosphor. The enhancement of excitation and emission intensity of the ceramic can also be attributed to the complete crystallization of ceramics, as plenty of defects would exist on both the particle surface and in the lattice due to the small particle size and relatively poor crystallinity of the powders. Defects will lead to the energy loss during the light absorption and emission, which in turn decrease the intensity of the excitation and emission.

Figure 5(a) and (b) show the excitation spectra of LuSAG/Tb(5%) phosphor and transparent ceramic, respectively. It was noted that the spectra distinctly differ from that of LuAG/Tb(5%) samples. They are characterized by an asymmetrical broad band with wavelength ranging from 220 to 340 nm. And they could be deconvoluted into many Gaussian-shaped bands, represented as dotted lines in Fig. 5 (a) and (b). As indicated by the comparison of Figs. 4(a), 5(a) and 5(b), the excitation spectra of LuSAG/Tb(5%) phosphor and transparent ceramic were also can be attributed to the Tb^{3+} 4f → 5d absorptions. Compared with that of LuSAG/Tb phosphor, the excitation spectrum of LuSAG/Tb ceramic shows integrated red shift in addition to the enhancement of all peak intensity caused by the significant increased crystallinity and density of ceramics. The emission spectra of the Tb^{3+} 270-nm excitation in LuSAG/Tb(5%) phosphor and LuSAG/Tb(5%) ceramics were showed in Fig. 5(c). There is no difference between the spectra of LuSAG/Tb and LuAG/Tb except for the peak intensity, as Tb^{3+} is not sensitive to the crystal field. It is very interesting to note that when Sc was introduced in the LuAG/Tb lattice, the emission intensity of both LuSAG/Tb phosphor and ceramic can be enhanced significantly as compared with that of LuAG/Tb, and such an enhancement of the luminescent intensity by the introduction of Sc into the LuAG/Tb is more effective for the transparent ceramic than phosphor powder. It should be pointed out that both the emission spectra of LuSAG/Tb phosphor and ceramics (Fig. 5c) were not recorded at the wavelength of maximum excitation strength to avoid the strongest peaking exceeding the up-limit of the spectrometer. By comparing the intensities of relatively weak peaks between LuAG and LuSAG under the excitation at the wavelength of maximum excitation strength, it could be estimated that the luminescent intensity of LuSAG/Tb ceramic is 150% higher than that of LuAG/Tb.

The luminescent enhancement of both phosphors and ceramics of LuSAG/Tb over LuAG/Tb can be explained as

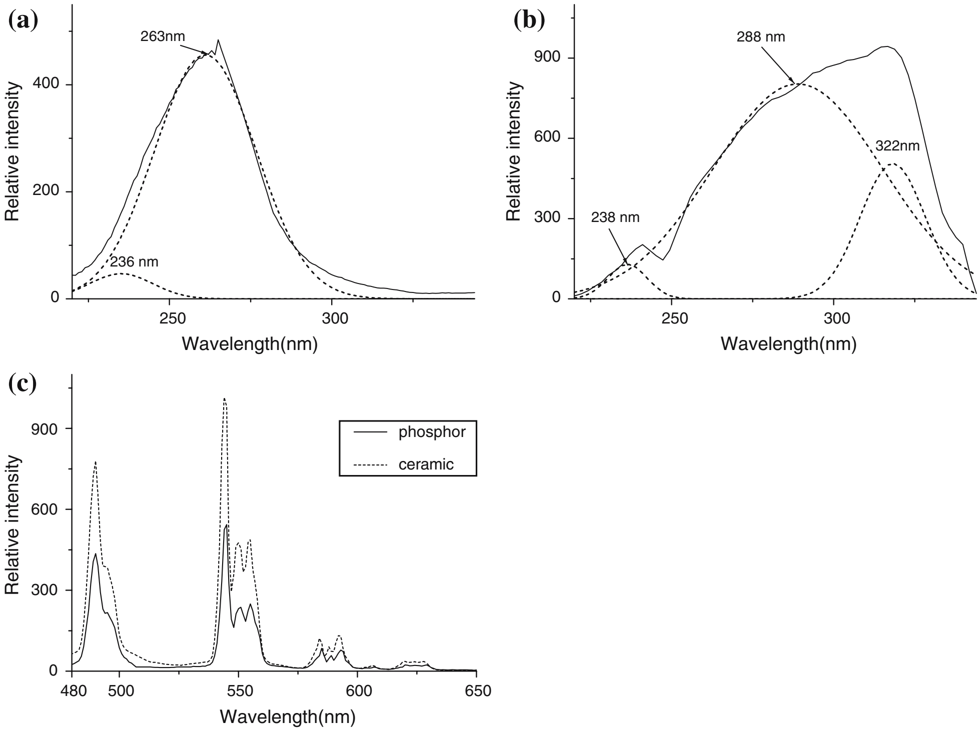

Fig. 5 Photoluminescence spectra of LuSAG/Tb($Tb_{0.15}Lu_{2.85}Sc_2Al_3O_{12}$): (**a**) excitation spectra of phosphor (λ_{em} = 480 nm); (**b**) excitation spectra of ceramic (λ_{em} = 480 nm); (**c**) emission spectra (λ_{ex} = 270 nm)

followings. First, although the phosphors were calcined in air, a large amount of defects, especially oxygen vacancies, exist in them. The highly reducing atmosphere present in H_2 furnace during the sintering process caused substantial discoloration of the material, leading to a darkish color of ceramics. This discoloration mainly associated with oxygen vacancies, occurred in ceramic [12]. When Al^{3+} was partially substituted with Sc^{3+}, which has a larger ion size, the host lattice is more closely packed by the Sc doping. The formation of the defects, especially oxygen vacancies, can be suppressed by limited ionic movement [13]. In our experiment, the discoloration always exists in LuAG:Tb transparent ceramics, however, near colorless LuSAG:Tb transparent ceramics can be obtained due to the introduction of Sc. In other words, the doping of Sc into the host lattice is effective for reducing the density of oxygen vacancies and preventing the formation of color centers. Second, the enhancement of luminescent intensity may also be attributed to the change of lattice parameter. Because the radius of Sc^{3+} is larger than Al^{3+}, the substitution of Sc^{3+} in the octahedrally coordinated site of Al^{3+} will cause the increase of lattice constant. The complete substitution of Sc^{3+} into the octahedral site of Al^{3+} in LuAG increase the lattice parameter from 11.9164 for $Lu_3Al_5O_{12}$ to ~12.1179 for $Lu_3Sc_2Al_3O_{12}$ [14, 15]. The distance of activators in dodecahedral site increases accordingly, which could in turn suppress the concentration quenching effect. For the relatively high concentration doping, the luminescence intensity increases significantly with the decrease of the concentration quenching effect.

Conclusion

In this paper we have demonstrated the synthesis of the LuAG/Tb and LuSAG/Tb phosphor powders by the coprecipitation technique that shows high sinterability. The average crystalline sizes of the resulting powders are in the range from 20 to 30 nm. Such powders can be easily sintered into transparent LuAG/Tb and LuSAG/Tb ceramics at 1850 °C in H_2 atmosphere without any additives. The doping of Sc into LuAG is effective for reducing the density of oxygen vacancies and suppressing the concentration quenching effect, which in turn enhances the luminescent intensity of the phosphor and transparent ceramic.

References

1. Yamamoto H, Matsukiyo H (1991) J Lumin 48–49:43
2. Ustel TJ, Nikol H, Rhonda C (1998) Angew Chem, Int Ed 37:3084
3. de Pooter JA, Bril AB (1975) J Electrochem Soc 122:1086
4. Papagelis K, Ves S (2003) J Phys Chem Solids 64:599
5. Kasamatsu T, Sekita H, Kuwano Y (1999) Appl Opt 38:5149
6. Hart DW (1996) Opt Lett 21:728
7. Ogino H, Yoshikawa A, Lee J-H, Nikl M, Solovieva N, Fukuda T (2003) J Cryst Growth 253:314
8. Ryskin NN, Dorenbos P, van Eijk CWE, Batygov SKh (1994) J Phys Condens Matter 6:10423
9. Oginoa H, Yoshikawaa A, Leea J-H, Niklb M, Solovievab N, Fukuda T (2003) J Cryst Growth 253:314
10. Yikun L, Danyu J, Tao F, Jianlin S J Mater Res (to be published)
11. Ji Y-m, Jiang D-y, Shi J-l (2005) Mater Lett 59:868
12. Zych E, Brecher C, Wojtowicz AJ (1997) Lingertat H 75:193
13. Matsukiyo H, Toyama H, Uehara Y, Yamamoto H (1997) J Lumin 72–74:229
14. Kuwanoa Y, Sudab K, Ishizawab N, Yamada T (2004) J Cryst Growth 260:159
15. Brandle CD, Barns RL (1973) J Cryst Growth 20:1